

Experiment on Unsymmetrical Subharmonic Oscillations in a Symmetrical Three-Phase Circuit

By

Kohshi OKUMURA and Tsutomu YAMADA

(Received March 31, 1995)

Abstract

This paper presents several results of experiments on the generation of 1/3-subharmonic oscillations in a nonlinear symmetrical three-phase circuit. Particular attention is paid to the generation of unsymmetrical modes. Furthermore we describe a switching phase controller essential to the generation of the subharmonic oscillations in the experimental circuits.

1. Introduction

The model of the three-phase circuit is composed of capacitors, resistors, symmetrical three-phase voltage sources and the wye-delta connected transformers of which magnetizing characteristics are given by the nonlinear function of magnetic flux-interlinkages. We have shown analytically by extending Krylov, Bogoliubov and Mitropolsky's asymptotic method that the nonlinear symmetrical three-phase circuit may generate three modes of 1/3-subharmonic oscillations [1, 2, 3]. These synchronization modes are denoted as S1, S2 and S3; mode S1 is the 1/3-subharmonic oscillation caused by one of the three nonlinear inductors, S2 by two nonlinear inductors and S3 by three nonlinear inductors. The modes S1 and S2 are unsymmetrical and S3 is symmetrical.

The objective of this paper is to ensure the generation of these symmetrical and unsymmetrical synchronization modes by means of real experiment.

2. Experimental Three-Phase Circuit

We make up the experimental three-phase circuits shown in Fig. 1. The nonlinear elements are three inductors. The data of the circuit elements are as follows:

Three-phase voltage sources: Three autotransformers are connected in a wye-connection without grounding of the neutral point. The data of each autotransformer are the following: capacity 20 kVA, maximum current 100 A, primary voltage 200 V, secondary

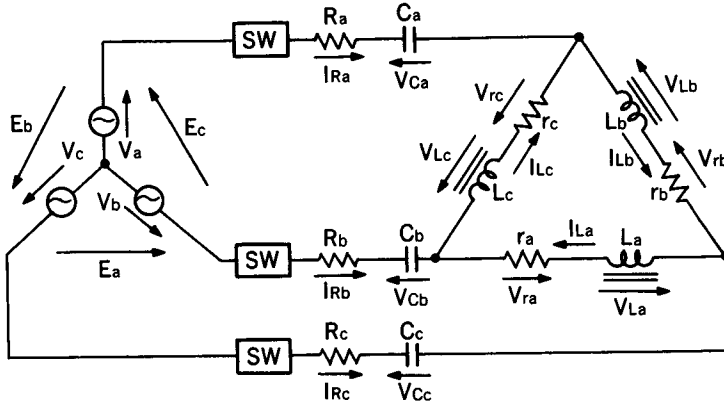


Fig. 1. Experimental nonlinear three-phase circuit. (SW is a thyristor switch. The phase of switching is controlled.)

voltage changeable from 0 V to 240 V. The frequency is 60 Hz.

The resistor R: Series connection of two winding resistors. Resistor 1: capacity 0.75 kW, maximum current 5 A, maximum resistance 30 Ω . Resistor 2: capacity 1.0 kW, maximum current 10 A, maximum resistance 10 Ω .

Resistors r in delta windings: resistance r is 2.0 Ω .

Switch: Semiconductor switch connected with SCR and power diode in parallel.

Capacitor: 21 M.P. condensers (W.V. 500 V 30 μf) are used to increase the capacity from 7.5 μf to 472.5 μf . Each capacitor can be charged with DC voltage sources to set the initial voltages.

Nonlinear inductors: Cut-cores are used. The diameter of windings is 1.1 mm.

3. Switching Phase Controller

Different types of oscillations such as S1, S2 and S3 may be generated. They depend on the value of the initial conditions. The initial charging voltage across capacitor C is supplied from the DC voltage sources. With respect to the other initial condition, i.e. the phase angle at which the oscillation starts, an ordinary switch is not adequate to create accurate timing because it has a time lag which may not be constant for every operation. The voltages must always be applied to the three-phase circuit at a predetermined phase angle θ of the voltage wave. Hence we make up the switching phase controller. The block diagram is shown in Fig. 2.

The pulse generator generates a rectangular wave with a period of $T=1/60$ second. The rectangular wave is synchronized with the frequency of the voltage source (60 Hz).

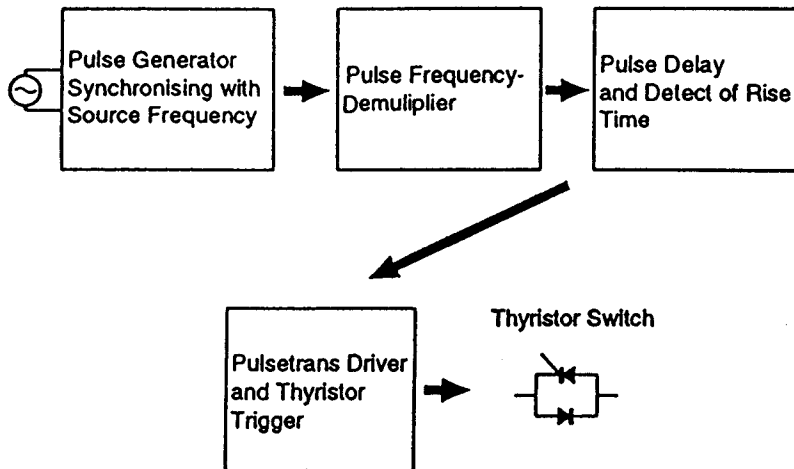


Fig. 2. Configuration of switching-phase controller.

The circuit uses the comparator. In the pulse frequency-demultiplier one pulse per 4 seconds is generated. In the third block the pulse trigger is delayed to close the switch. This part varies the timing to send the trigger pulse to the gate of the thyristor. The pulse width is limited to pass the pulse transformers. Hence, a monostable multivibrator is used to create a pulse with a shorter width. The DC voltage source in Fig. 3 supplies the DC current to SCR switches. The trigger coming from the CMOS circuit is not so high that it is amplified as high as the pulse transformer is driven. The pulse width of the trig-

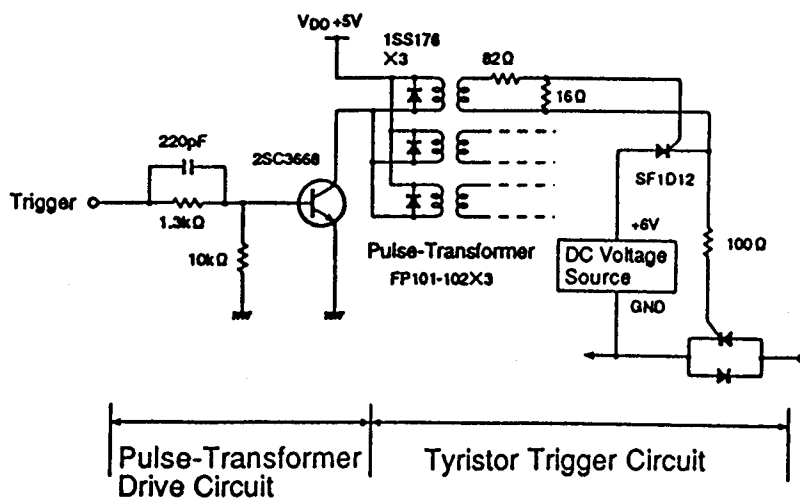


Fig. 3. The thyristor driver part of phase controller.

ger output is 30 micro seconds. The diodes in the primary windings protect the transistor by absorbing the inverse mmf of the pulse transformers.

4. Test Results of Phase Controller

The phase controlled circuit is tested by setting several switching phases. Some results are shown in Fig. 4. The switching phase θ is set to 0 and 90 degrees. The DC voltage 50 V is due to the charged voltage of the capacitor. We have satisfactory results.

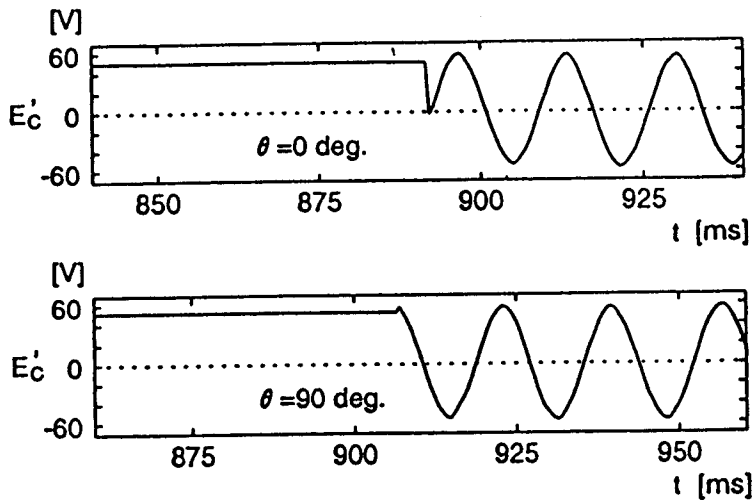


Fig. 4. Several results of phase control. (The voltage E_c' is the line voltage between a and b-phase SW.)

5. Magnetizing Characteristics of Nonlinear Inductors

The magnetizing characteristics of the three nonlinear inductors is measured. The magnetizing characteristics is given in Fig. 5. The three nonlinear inductors have almost the same characteristics.

6. Experimental Method

First we adjust equally the line voltages E_a , E_b and E_c by setting V_a , V_b and V_c to an equal voltage and also set the resistance R . The line voltage is denoted as E_Δ ($=E_a=E_b=E_c$). Second, all the capacitors are discharged and the capacitances C ($=C_a=C_b=C_c$) are set. In the next step, the capacitors in one phase, for example the a-phase, are charg-

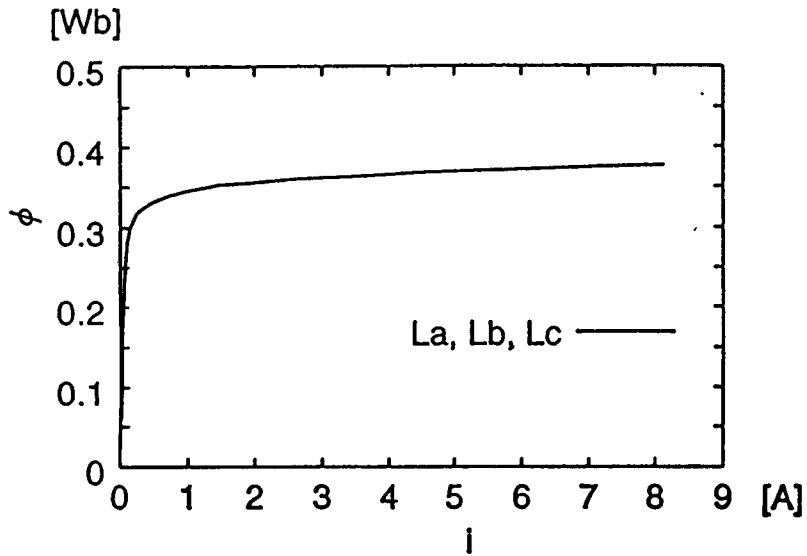


Fig. 5. Magnetizing characteristics of nonlinear inductors. (ϕ : Flux-interlinkage; i : Exciting current)

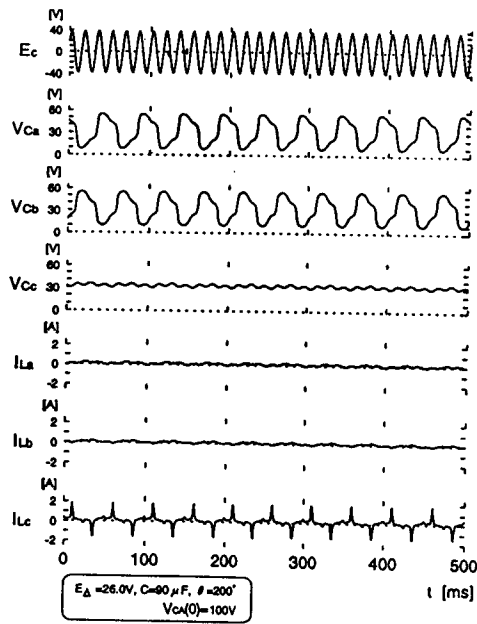


Fig. 6. Mode S1. $E_{\Delta} = 26.0 V$, $C = 90 \mu F$, $\theta = 200^\circ$, $V_{Ca}(0) = 100 V$.

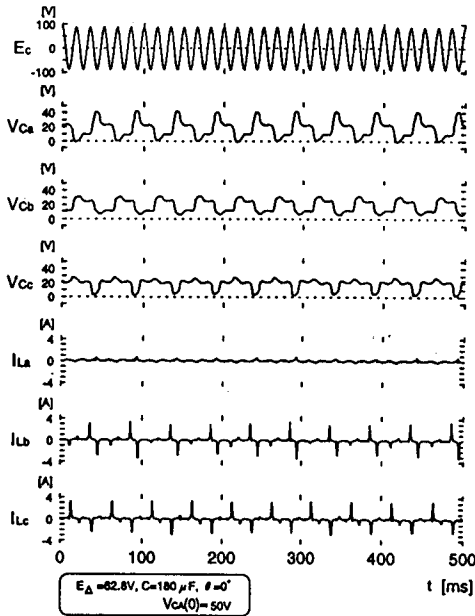


Fig. 7. Mode S2. $E_{\Delta} = 62.8$ V,
 $C = 180 \mu\text{F}$, $\theta = 0^{\circ}$, $V_{CA}(0) = 50$ V.

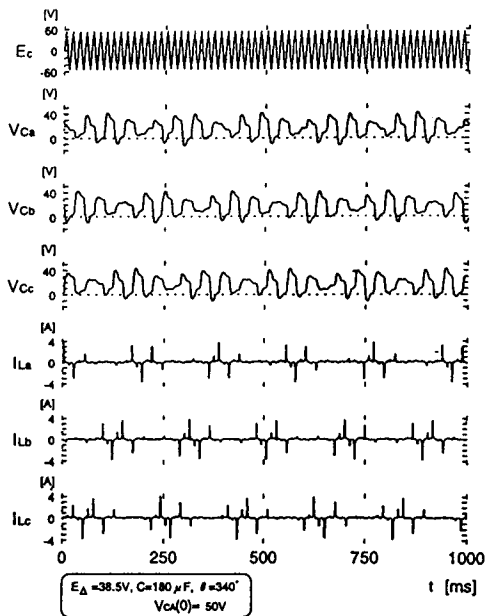


Fig. 8. Mode S3. $E_{\Delta} = 38.5$ V,
 $C = 180 \mu\text{F}$, $\theta = 340^{\circ}$, $V_{CA}(0) = 50$ V.

ed up to an initial voltage. After setting the switching phase, the trigger shots the gate of SCR and the circuit is switched on.

7. Experimental Results

The three modes of 1/3-subharmonic oscillations which are expected by the analysis can be generated. These waveforms are shown in Fig. 6 to Fig. 8. The waveforms of the currents through the nonlinear inductors i_{La} , i_{Lb} and i_{Lc} reveal the three modes. The regions where the three modes of 1/3-subharmonic oscillations are generated are illustrated in Fig. 9.

The frequency components of S1 mode are 20, 60, 100 Hz and so on. The highest component is 20 Hz. The even components (2/3, 4/3 and so on) can be found a little. The frequency components of S2 mode are 20, 40, 60, 80, 100 Hz and so on. The even components are stronger than mode S1. The S2' mode which is a different type of mode S2 is not found by mathematical analysis. The frequency spectrum is quite different from that of mode S2. However it is noted that mode S2' has the strong components 20, 60, 100 Hz and so on. Unlike S2 mode, between these components there can be found various kinds of frequency components. The 1/3-subharmonic oscillation of the S2' mode is chaotic.

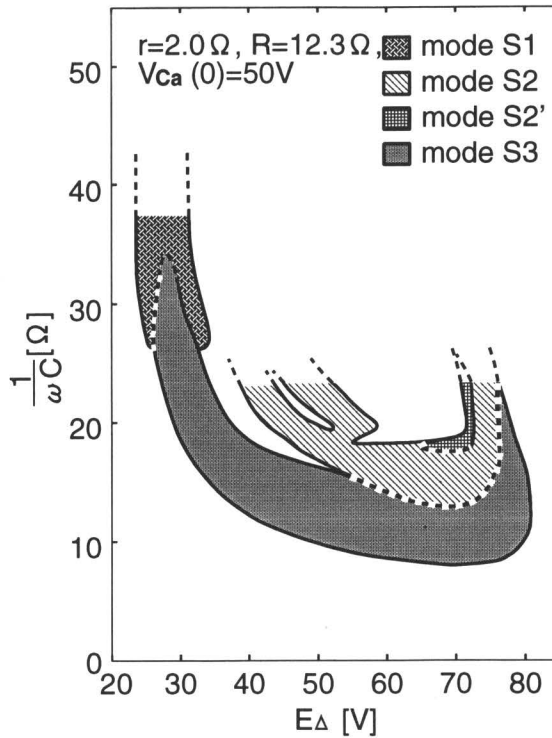


Fig. 9. The regions of 1/3-subharmonic oscillations.

Mode S3 accompanies the beats. The frequency components of the S3 mode are about 18, 23, 28, 32 and so on. This experimental fact is a little different from the analytical result obtained under the assumption that the 1/3-subharmonic oscillations are in synchronism. In the area where the source voltage E_{Δ} is around 30 V there exists an overlapping area of mode S1 and S3. In this region a transition from mode S1 to S3 is impossible. Once mode S1 is fixed, it is kept as it is. However, a transition from mode S3 to S1 is possible. If voltage E_{Δ} is increased, mode S3 is changed to mode S1. The transition between mode S1 and S3 is irreversible. If resistance R is increased, then the region of mode S1 fades away and there remain modes S2, S2' and S3. If we increase resistance R further, then we have only one region, mode S3. Hence the symmetrical mode S3 is most common in this experimental circuit. We can conclude that as resistance R becomes smaller the unsymmetrical mode comes to be seen.

8. Concluding Remarks

In order to compare the analytical results of the $1/3$ -subharmonic oscillations with those in the real circuit, we have made up the experimental nonlinear symmetrical three-phase circuit. Particular attention has been centered on the symmetrical and unsymmetrical modes of the $1/3$ -subharmonic oscillations which are analytically confirmed to be generated. However, mode $S2'$ can not be ensured by the analysis. More precise analysis is now going to be performed.

Acknowledgement: One of the authors expresses his sincere thanks to professor emeritus Akira Kishima of Kyoto University who has led his way.

References

- [1] K. Okumura and N. Miyamoto; "Subharmonic Entrainment of Frequency in Nonlinear Three-Phase Circuits with Symmetry", Proc. of ISCAS '93, IEEE, pp. 2624-2627, 1993.
- [2] K. Okumura and A. Kishima; "Subharmonic Oscillations in Three-Phase Circuits," Int. J. Non-Linear Mechanics, Vol. 20, No. 5/6, pp. 427-438, 1985.
- [3] N. N. Bogoliubov and I. A. Mitropolsky; "Asymptotic Methods in the Theory of Nonlinear Oscillations," Fizmatgiz, Moscow (1958); Japanese translation by M. Masuko, Kyoritsu Pub., Co., Inc., (1958). M. N. Krylov and N. N. Bogoliubov; "Introduction to Non-linear Mechanics," Izv. Akad. Nauk USSR, Kiev (1937) (in Russian).